Multi-color Light Emitting Carbon Dots and their Application in Cell-imaging

M.Sc. Thesis

By

MITALI CHHABRA

DISCIPLINE OF CHEMISTRY

INDIAN INSTITUTE OF TECHNOLOGY INDORE

JUNE 2018

Multi-color Light Emitting Carbon Dots and their Application in Cell-imaging

A THESIS

Submitted in partial fulfillment of the
requirements for the award of the degree
of
Master of Science

by
MITALI CHHABRA

DISCIPLINE OF CHEMISTRY
INDIAN INSTITUTE OF TECHNOLOGY INDORE
JUNE 2018

INDIAN INSTITUTE OF TECHNOLOGY INDORE

CANDIDATE'S DECLARATION

I hereby certify that the work which is being presented in the thesis entitled **Multi-color Light Emitting Carbon Dots and their Application in Cell-imaging** in the partial fulfillment of the requirements for the award of the degree of **MASTER OF SCIENCE** and submitted in the **DISCIPLINE OF CHEMISTRY, Indian Institute of Technology Indore**, is an authentic record of my own work carried out during the time period from July 2017 to June 2018 under the supervision of Dr. Tridib Kumar Sarma, Assistant Professor, IIT Indore.

The matter presented in this thesis has not been submitted by me for the award of any other degree of this or any other institute.

Mitali Chhabra

This is to certify that the above statement made by the candidate is correct to the best of my knowledge.

Dr. Tridib K. Sarma

Mitali Chhabra has successfully given her M.Sc. Oral Examination held on

Signature of Supervisor of MSc thesis
Date:

Convener, DPGC
Date:

Signature of PSPC Member
Date:

Signature of PSPC Member
Date:

ACKNOWLEDGEMENTS

With great pleasure, I want to express my deep sense of gratitude to my excellent supervisor Dr. Tridib K. Sarma, for giving me this wonderful opportunity to pursue research and believing in my research abilities and me. His constant guidance, support and motivation have been immensely helpful to complete this M.Sc. project. His enthusiasm and dedication has inspired me so much. Further I would like to thank my PSPC members Dr. Anjan Chakraborty and Dr. Debasis Nayak for their valuable suggestions and support.

I wish to express my gratitude to Prof. Pradeep Mathur, Director, IIT Indore for his help and support.

I am grateful to Dr. Amrendra Kumar Singh (Head, Discipline of Chemistry, Indian Institute of Technology Indore) for his suggestions and guidance in various aspects. I am also grateful to Dr. Tushar Kanti Mukherjee, Dr. Sheikh M. Mobin, Dr. Suman Mukhopadhyay, Dr. Satya Bulusu, Dr. Apurba Kumar Das, Dr. Sampak Samantha, Dr. Biswarup Pathak, Dr. Sanjay Singh, Dr. Rajneesh Mishra and Dr. Chelvam Venkatesh.

I extend my deep thanks to the PhD students of my group, Neha Thakur, Daisy Sarma, Abhiram Panigrahi, Siddharth Jain and Biju Majumdar for their help and cooperation. I would also like to thank Dr. Sonam Mandani for her help. I also wish to thank Ms. Suman Bishnoi for her valuable time and help in biology experiment.

I would also like to thank technical staff from Sophisticated Instrumentation Center (SIC), IIT Indore, Mr. Kinny Pandey, Mr. Ghanshyam Bhavsar and Mr. Manish Kushwaha for their patience and timely technical support without which it was impossible for me to

complete my work. I would also like to thank Ms. Anjali Bandiwadekar, Mr. Rajesh Kumar and other library staff.

I personally want to extend my thanks to my friends Konika Thukral, Priyanka and all my batch mates.

Here, it is to be specially mentioned that, it has been wonderful to work with many PhD seniors during my M.Sc. On this occasion I would like to record my thanks to Sagnik Sengupta, Soumya Kanti De, Nishu Kanwa and Miraj for their generous co-operation and help.

Finally, I would like to express my thanks to IIT Indore for infrastructure and all others who helped and supported me directly or indirectly.

MITALI

DEDICATION

Dedicated to my family

Abstract

Carbon dots (C-dots), the tiny nano lights, have unfolded as an integral part of nanomaterial family in recent years. Several advantages, such as easy synthesis and purification methods from commonly available organic molecules, tunable optical properties by doping with other heteroatoms make C-dots a great biocompatible alternative to the traditional semiconductor quantum dots owing to very low toxicity and high photo stability.

In this work, we report the development of a one-pot synthetic strategy for multicolor light emitting N-doped carbon dots with high quantum yields of 29% (blue c-dots), 61% (green c-dots) and 74% (yellow c-dots). These C-dots with varying nitrogen content exhibited bright and stable photoluminescence. C-dots were synthesized solvothermally from a mixture of fumaric acid and o-phenylenediamine (o-PD) in one pot and could be separated via silica column chromatography. The separated C-dots showed emission over a large spectrum of visible light from violet, blue, green, dark green, peach, light yellow and yellow fluorescence. Among these multicolored Carbon dots, the three major components, namely blue, green and yellow emissive C-dots were further characterized by spectroscopic techniques like UV-Vis, FTIR, XPS, XRD and TEM. Although the C-dots with variable emission were not different morphologically (all the C-dots are approximately 2 nm in diameter), the amount of nitrogen doping into the graphitic core varied. This resulted in varied amount of ordered packing of the alkyl groups in the core and less amount of hydrophilic surface functionalities. All the three differently emitted C-dots were employed for the *in vitro* imaging of cancer cells under a single-wavelength light source.

TABLE OF CONTENTS

LIST OF FIGURES

LIST OF TABLES

NOMENCLATURE

nm	Nanometer
mmol	Millimole
a.u.	Arbitrary unit
°C	Degree Centigrade
mL	Millilitre
eV	Electron Volt
ns	Nanosecond
MHz	Mega Hertz
mg	Milligram

ACRONYMS

CND	Carbon Nano Dot
CD	Carbon Dot
CQD	Carbon Quantum Dot
PL	Photoluminescence
UV-Vis	Ultraviolet visible Spectroscopy
TEM	Transmission Electron Microscopy
HRTEM	High Resolution Transmission Electron Microscopy
SEM	Scanning Electron Microscopy
XRD	X-ray Diffraction
FTIR	Fourier Transform Infrared
XPS	X-ray Photoelectron Spectroscopy
TCSPC	Time-Correlated Single Photon Counting
o-PD	o-phenylenediamine
TLC	Thin Layer Chromatography
QY	QuantumYield

Chapter 1

Introduction

1.1. General Background

Materials in the nanometer dimension (typically between 1-100 nm) have found immense technological applications in various areas. The application potential of the nanomaterials originates from the fact that their optical, electronic, magnetic and surface properties vary considerably to the same material with micron- or mm-scale dimension. Therefore tremendous research efforts are paid towards generation of nanomaterials with tunable opto-electronic properties and are used as the building blocks for practical technology.

With the recent developments in the synthetic and technological tools, research interests have been developed in nanoparticle based devices that have led to their important applications in various fields.

1.2. The Nanocarbon family

Carbon has an ability to catenate that has resulted in the formation of a variety of compounds. It forms covalent bonds with other atoms in different hybridization states (sp, sp^2, sp^3). The various allotropes of carbon are diamond, graphite and buckminsterfullerene (C_{60}) out of which C_{60} was the first one to be isolated as carbon nanomaterial in 1985 [1]. Fullerenes have 20 hexagonal and 12 pentagonal rings and an icosahedral symmetry closed cage structure [2].

The other forms of carbon like carbon nanotubes, graphite, graphene, graphene oxide and carbon dots have also been extensively studied as nano-dimensional material. Carbon nanotubes (CNTs) are tiny tubes made of sheets of carbon arranged in hexagonal rings. Sumio Iijima of Japan

explored these CNTs as a material formed during carbon arc discharge [3]. In 2004, Novoselov et al. reported that graphene is a thin film of atomic size graphite [4]. These carbon nanomaterials, because of quantum confinement effect show interesting properties, which are not shown by their bulk members like diamond and graphite [5-8]. The lack of hydrophilic groups in these materials made their dispersibility in various solvents a difficult task [9-11].

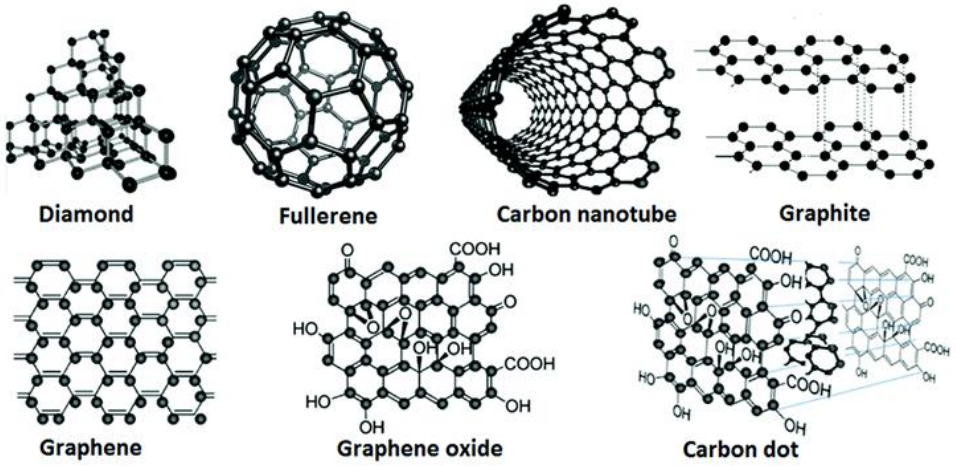

Figure 1.1 Various forms of carbon (adapted from reference 12)

1.3. Carbon nanodots (CNDs)

Carbon Nano Dots (CNDs) or Carbon dots (CDs), as an important part of carbon nanomaterial family have acquired massive research interests because of their unique optical properties, high photo stability and low cost that are lacking in other nano-allotropic forms of carbon [13-15]. Carbon dots are superior in terms of low toxicity and outstanding biocompatibility when compared to the traditional semiconductor quantum dots [16-18]. Xu *et al.* accidentally discovered these in 2004 while purifying single walled CNTs [19].

Carbon dots (C-dots) are fluorescent carbonaceous nanomaterial that contains oxygen, nitrogen or any other heteroatom functionalized groups on the outer surface and the inner core of carbon is sp^2 and sp^3 hybridized

carbon atom network [20]. These are usually below 10 nm in size and are spherical shaped [21].

C-dots can be synthesized from various cost effective precursors following simple methods that can result in a great variety of carbon dots with functionalization, biocompatibility and low toxicity [14]. Most of the carbon dots have chemical inertness and high stability along with resistance to photo bleaching [14]. The synthetic routes for C-dots can be classified into two main groups: top-down and bottom-up methods. A top-down approach is mainly the breaking of larger carbon materials such as graphite, coal, CNTs, etc. to small nanoparticles which is carried out by laser ablation, oxidative cutting, plasma treatment, chemical oxidation etc. [22-24]. On the other hand, bottom-up method makes use of molecular precursors that upon treatment lead to formation of C-dots [25,26]. The resulting C-dots are purified and separated by various techniques. The C-dots can be further functionalized or incorporated with other materials to form nano-composites for different applications [27,28]. C-dots mainly contain carbon, hydrogen and oxygen as their constitutive elements but can be doped with other atoms like nitrogen, phosphorous and boron depending on the precursors [29]. Doping of C-dots with different heteroatoms is an effective method to tune their optical properties.

The variety of techniques (chemical, bottom-up, top down) adopted for the production of C-dots from a variety of carbon precursors show that there are limitations with respect to controlled particle size distribution of C-dots, a main criteria for tunable optical properties.

1.4. Absorption and Photoluminescence of C-dots

The most interesting property of C-dots is their intrinsic photoluminescence (PL) and exciting at different wavelengths can control their emission. However, the fluorescence mechanism is not completely understood yet. In most studies, the PL emission spectra of Carbon dots

are broad with a maxima at certain wavelength implying that CDs have non-homogeneous chemical structures or contains diverse fluorophores which could be either surface-located or core-embedded [20]. Because of the different synthetic methods and ingredients, it is very difficult to control the luminescence of C-dots and have an insight into the mechanism [30-32].

In metal-based quantum dots, the fluorescence emission can be easily tuned by changing the size of quantum dots but the PL mechanism in carbon dots is complex. Till date, there have been only a few successful reports of Carbon dots with tunable PL. For example, Hu *et al*. produced a sequence of C-dots by varying the reagents and observed that epoxides and hydroxyls on the surface of C-dots were accountable for the red shift of fluorescence emission [33]. Lin *et al*. synthesized blue, green, and red emissive C-dots by solvothermally treating different isomers of phenylenediamine and observed that the PL red shift was due to different particle size and the nitrogen content of the C-dots [34]. Pang and coworkers also prepared a sequence of C-dots by changing the synthetic conditions and attributed that red shift in emission peaks was due to quantum size effects and surface states [35]. Although C-dots with tunable photoluminescence have been successfully obtained but the conclusion and mechanisms are still unclear and doubtful. From the aforementioned studies, it is clear that the PL mechanisms were not persuasive because there were divergent factors controlling the emission of C-dots [36-39].

Chapter 2

Review of past work

2.1. Previous Reports

Recently, phenylenediamines [three isomers: *o*-phenylenediamine (o-PD), *m*-phenylenediamine (m-PD), and *p*-phenylenediamine (p-PD)] have emerged out as significant precursors for preparing nitrogen doped carbon dots. For example, Liu and co-workers reported yellow fluorescent carbon dots from o-phenylenediamine for detection of Fe^{3+} and H_2O_2 attributing the photoluminescent behavior to the amino or hydroxyl groups present on the surface [40]. Lin *et al.* synthesized C-dots with blue, green, and red emission from the different isomers of phenylenediamines and found that the PL red shift was because of different particle size and nitrogen content [34]. In 2016, Xiong *et al*. reported one pot hydrothermal synthesis of full-color light emitting C-dots from blue to red with urea and p-PD ascribing the shift in emission peaks to the oxidation of the surface groups [41].

2.2. Objective of the Thesis

In the current study, we report a facile one pot solvothermal preparation of multicolor photo luminescent C-dots having blue (QY=29%), green (QY=61%) and yellow (QY=74%) as the major emission components along with pink, dark green and peach from a mixture of fumaric acid and o-PD as the precursor. The multi-emissive C-dot mixture showed excitation dependent emission. The C-dots with various emissions could be separated via silica column chromatography using ethyl acetate-hexane as eluent. Due to different polarity of the C-dots, the separation was feasible and the nanodots with narrow emissive distribution could be separated. After purification, C-dots exhibit excitation-independent luminescence from blue to peach, which is characterized by a single excitation peak and a tri-exponential lifetime. The C-dots were

successfully applied for cell imaging by virtue of their stable photoluminescence and high quantum yield.

The cis-form of fumaric acid i.e. maleic acid was also experimentally tested for the same solvothermal treatment with o-PD. Unlike fumaric acid, maleic acid did not produce multicolor fluorescent spots on Thin Layer Chromatography (TLC).

The purpose of the study was to understand the mechanism of excitation dependent emission properties of nitrogen doped C-dots and to separate the mixture into individual C-dots with narrow excitation-independent emissive entities.

Chapter 3

Instrumentation and Experimental Section

3.1. Instrumentation

A Varian Cary 100 Bio spectrophotometer was used for UV-Visible measurements. X- ray diffraction patterns (XRD) were obtained on a Rigaku, Ultima VI powder X-ray diffractometer using thin films. FTIR spectra were recorded in KBr pellet using a Bruker Tensor 27 instrument. Emission spectra were recorded using a fluoromax-4p fluoro-meter from Horiba (Model: FM-100). X-ray diffraction patterns (XRD) were obtained on a Bruker D8 Advance diffractometer with a Cu Kα source (wavelength of X-rays was 0.154 nm). A JEOL JEM-2100 microscope was used to obtain the transmission electron microscopy (TEM) images at an operating voltage of 200 kV. FTIR spectra were recorded in KBr pellet using a Bruker Tensor 27 instrument. The time resolved fluorescence studies were performed on Horiba Yvon (model: Fluorocube-01-NL), a nanosecond time correlated single photon counting (TCSPC) system.

3.2. Instrumentation Techniques

3.2.1. UV-Visible Spectroscopy: It refers to absorption spectroscopy in the ultraviolet-visible spectral region. The absorption in the visible range directly affects the interpreted color of the chemicals involved. Absorption measures transitions from the ground state to the excited state. A beam source emitting light of multiple wavelengths is focused on a sample. When the sample is striked upon, the photon that matches the energy gap of the molecule is absorbed to excite the molecule.

3.2.2. Fluorescence Spectroscopy: In this spectrochemical method, the analyte is excited with a certain wavelength and it emits the radiation of a different wavelength. When a molecule absorbs excitation wavelength, the molecule gets excited from the ground electronic state to a vibrational

level in one of the excited electronic states. From this excited state, the molecule relaxes via several processes and one of these processes is fluorescence that results in the emission of light.

3.2.3. Fourier Transform Infra-Red (FTIR) Spectroscopy: FTIR is based on the fact that the bonds of the molecules absorb light in the infrared region. The frequency range is measured over the range of 4000 – 600 cm^{-1}. The infrared spectrum of a sample is recorded by passing a beam of infrared light through the sample. Absorption occurs when the vibrational frequency of a bond is same as the frequency of IR.

3.2.4. X-ray Photoelectron Spectroscopy (XPS): Photo-ionization is the basic principle of photoelectron spectroscopy. In order to study the electronic states of the surface region, it analyses the kinetic energy distribution of the emitted photoelectrons. Soft X-rays with a photon energy of 200-2000 eV are used to examine core- levels. The emitted electrons are dispersed by an electron energy analyzer according to their kinetic energy and the flux of emitted electrons of a particular energy is measured. This is done in a high vacuum environment so that the emitted photoelectrons are analyzed without any disturbance.

3.2.5. X-ray Diffraction: In this technique, X-rays are used on thin films for structural characterization of the material. The source of diffractometer produces waves at a known frequency. XRD operates under the assumption that the sample is randomly arranged. Upon striking of X-rays, the atoms of the sample behave as a diffraction grating and produce bright spots at particular angles. Diffraction allows for rapid and non-destructive analysis of mixtures with multiple components.

3.2.6. Transmission Electron Microscopy (TEM): In this, a beam of electrons passes through the sample and it provides information on the internal structure of the samples unlike SEM which gives idea about the outer / surface morphology. It is based on transmitted electron or produces

images by detecting primary electrons transmitted from the sample. TEM can show many characteristics of the samples, such as morphology, crystallization, stress or even magnetic domains whereas SEM only shows the morphology of samples. TEM has a better resolution than SEM.

3.2.7. Time-Correlated Single Photon Counting (TCSPC): TCSPC provides the information of lifetime of samples. We used a picosecond TCSPC system. The repetition rate was 5 MHz. The signals were collected at an angle (54.70^{o}) polarization using the photomultiplier tube as the detector with a dark count of less than 20 cps. The instrument response function value of the setup is 140 ps. The fluorescence decay was described as a sum of exponential functions:

$$D(t) = \sum_{i=1}^{n} a_i \exp\left(\frac{-t}{\tau_i}\right)$$

Where *D(t)* is the normalized fluorescence decay. τ_i are the fluorescence lifetimes of various fluorescent components and a_i are the normalized pre-exponential factors. The amplitude weighted lifetime is given by:

$$\langle \tau \rangle = \sum_{i=1}^{n} a_i \tau_i$$

The fit was decided by reduced Chi square (χ^2) values and their corresponding residual distribution. In order to obtain the best fitting in all of the cases, χ^2 was kept near to unity.

3.3. Experimental Section

3.3.1. Materials Required: Fumaric acid, o-phenylenediamine and ethanol (UV and HPLC grade >95% pure) were purchased from Sigma Aldrich.

3.3.2. Synthesis of C-dots: Fumaric acid (0.86 mmol, 100 mg) and o-

phenylenediamine (1.72 mmol, 186.3 mg) were dissolved in 10 mL of ethanol and the reaction mixture was transferred into a Teflon-lined stainless steel autoclave. The reaction was heated at 180 °C for 15 h and then cooled to room temperature. The resultant solution was purified via silica column chromatography using a mixture of ethyl acetate and hexane as the eluent. The obtained fragments (C-dots) with different fluorescence were dispersed in ethanol.

3.3.3. Separation of C-dots: Eight samples with marked fluorescence features were collected after purification through silica column chromatography. These exhibited colors ranging from blue to peach, when excited under UV light of 365 nm. A slow flow rate was maintained so as to avoid mixing of different C-dots and the polarity of the eluting solvents was progressively increased. The purified Carbon dots were dried and dispersed in ethanol for use. Three major samples exhibiting blue, green and yellow fluorescence were selected for further characterization.

3.3.4. Quantum Yield Measurement: The quantum yield (QY) of all the three C-dots was calculated using the following equation

$$\Phi = \Phi_R * I/I_R * OD_R/OD * \eta/\eta_R^2$$

Where Φ and I are the quantum yield and measured integrated emission intensity respectively, η is the refractive index and OD is the optical density. The subscript R refers to the reference fluorophore of known quantum yield. Quinine sulfate in 0.1 M H_2SO_4 (quantum yield 54%) was chosen as a standard for sample A excited at 320 nm. Fluorescein in Ethanol (Φ_R=0.79) was chosen for sample B and excited at 440 nm. For sample C, Rhodamine B with Φ_R=1.0 was taken as reference in ethanol with excitation wavelength of 380 nm. In all cases, absorption was kept $\leq$ 0.1.

Chapter 4

Results and Discussion

4.1. Synthesis and Characterization of Carbon Dots

Carbon dots were synthesized from a mixture of fumaric acid or its isomer maleic acid and o-phenylenediamine (o-PD) as the carbon and nitrogen source respectively under high-temperature solvothermal conditions as described in the experimental section. Then, the resulted products were observed under UV light. The product solution of maleic acid and o-PD pair emitted blue-green fluorescence. On the other hand, solvothermal treatment of a mixture of fumaric acid and o-PD resulted in C-dots with yellow-orange fluorescence in high yield (**Figure 4.1.A**). We further controlled the molar ratio between fumaric acid and *o*-phenylenediamine and at a ratio of 1:2, formation of yellow-orange C-dots were observed which showed strongest fluorescence among all the combinations. At other ratios like 1:1, 1:3 and 1:4, the fluorescence occurred at variable colors from bluish green to pale yellow. In a similar way, the optimal temperature and reaction time were found to be 180 °C and 15 h, respectively.

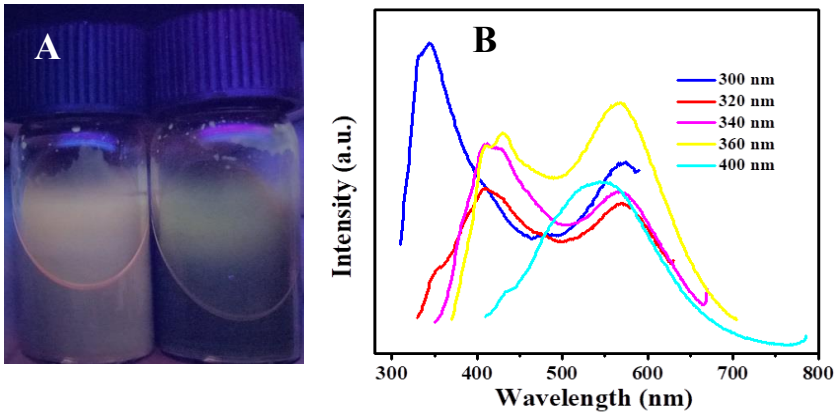

Figure 4.1. (A) Digital images of the prepared reaction mixtures fumaric acid with o-PD (left) and maleic acid with o-PD (right) under UV light. (B) Fluorescence spectra of Fumaric acid and o-PD mixture when excited at variable wavelengths.

The C-dots obtained from a mixture of fumaric acid and o-PD showed emission maximum at 343 nm, with several humps at 411, 430 and 569 nm (**Figure 4.1.B**). The C-dots also showed excitation dependent emission properties and the maximum emission was observed while excited at 300 nm. The presence of multiple peaks in the emission spectra suggested that the fluorescence was originated from multiple C-dots having variable emission. This prompted us to investigate whether it will be possible to separate the C-dots with different emission properties and study their physio-chemical properties.

We first observed the separation of the C-dot solution by thin layer chromatography (TLC). When the C-dots were run on a TLC plate using a ethyl acetate-hexane mixture as eluent, various multi-colored fluorescent spots including blue, green, dark green, pink, peach and yellow, could be separated. This suggested that the synthesized C-dots were actually a mixture of C-dots having different emission (**Figure 4.2.**). This prompted us the fractionation of these carbon dots using silica column chromatography by maintaining a slow flow rate to avoid the mixing of carbon dots. The obtained carbon dots were dried and dispersed in ethanol for further analysis. Three samples namely blue, green and yellow were further characterized by FTIR, XPS, TEM and other spectroscopic techniques. These samples were labeled as samples A, B and C respectively.

Afterwards, maleic acid, fumaric acid and o-PD were put under the same solvothermal conditions individually. The emission of both maleic acid and fumaric acid was in the blue region whereas o-PD yielded green fluorescence.

4.1.1. UV-Visible Absorption and Photoluminescence Spectra

The UV−vis absorption spectra of the three selected samples, as shown in **Figure 4.3.**, is almost similar in the region of 200−300 nm which

corresponds to the π–π* transitions of C=C and C=N bonds, from the polyaromatic rings in the C-dots. The absorption is different in the lower-energy region with bands located at 296 nm, 386 nm and 457 nm for A, B and C respectively showing the presence of different surface states or extended conjugation. The emission of the three samples was excitation-independent (**Figure 4.3.**).

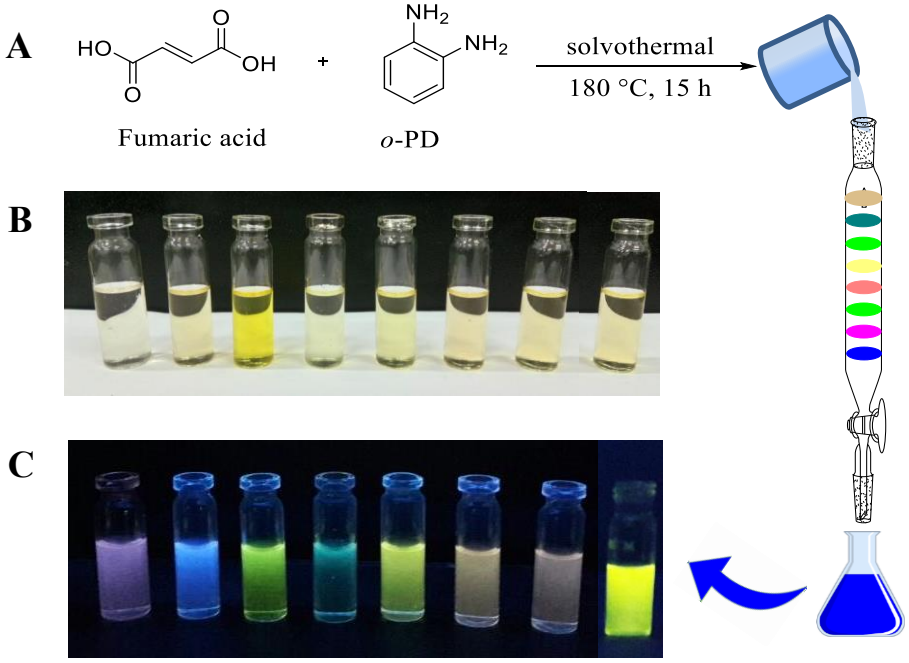

Figure 4.2. (A) Schematic representation of one pot synthesis and purification path for C-dots with distinct characteristics. (B and C) The purified eight samples under daylight and under 365 nm UV light.

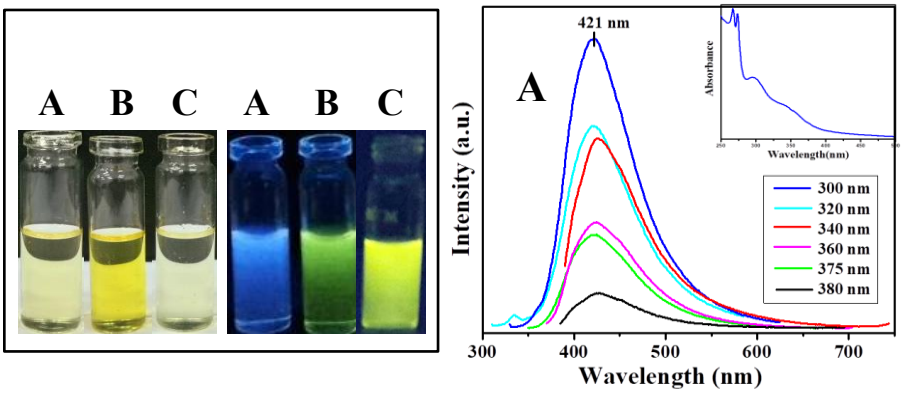

Figure 4.3. Digital image of samples A, B and C in ethanol under daylight (left) and UV light (right). (A) PL spectra of sample A and absorption (inset).

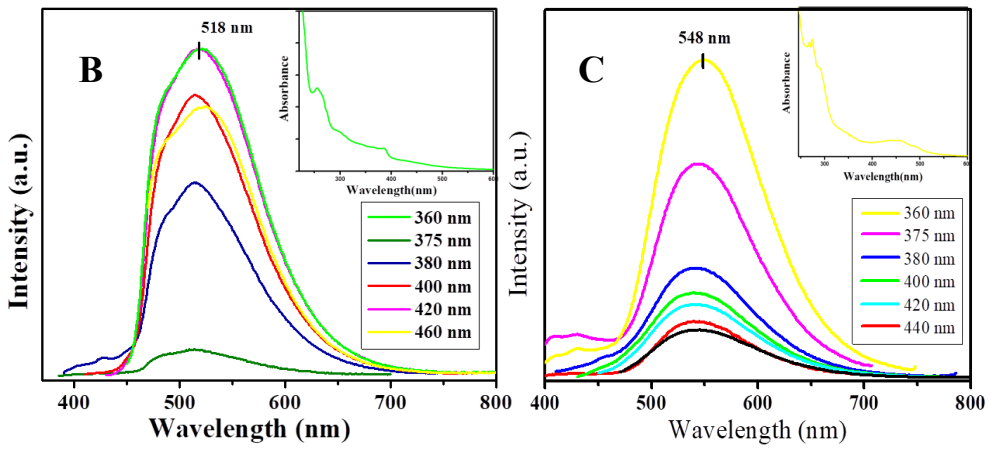

Figure 4.4. B and C show the PL emission spectra under excitation with different wavelengths and absorption curve (inset).

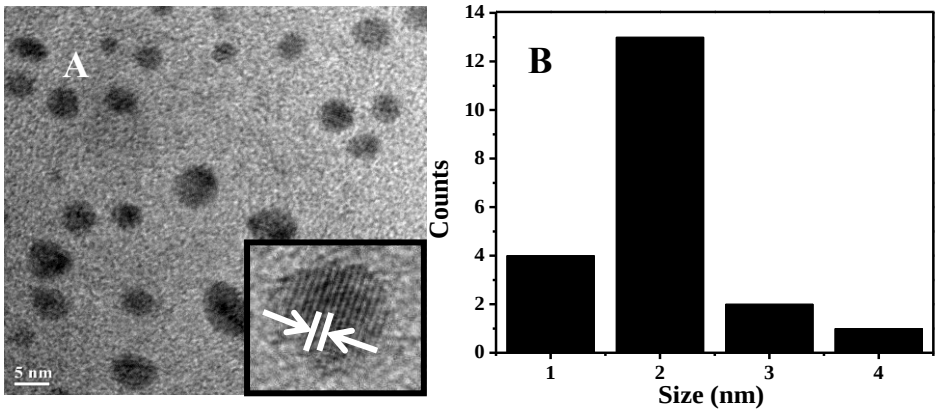

Figure 4.5. (A) TEM and HRTEM (inset) image of sample A. The scale bar represents 5 nm. (B) Histogram of the particle size distribution of sample A.

4.1.2. Morphology and structure characterization

The morphology of CDs was studied using TEM. The images of sample A reveal the presence of well-dispersed spherical carbon nanoparticles with an average particle size of approximately 2 nm (**Figure 4.5.**). The high-resolution (HR) TEM image provided in the inset show that the CDs exhibited well-resolved lattice fringe with a spacing of 0.56 nm, which is larger than that of the bulk graphite (0.33 nm).

4.1.3. XPS analysis

XPS analysis was done to further investigate the surfaces of these three samples. The full spectra presented in **Figure 4.6.** show three typical peaks: C 1s (284.4 eV), N 1s (399.6 eV), and O 1s (531.7 eV). This shows that all the three samples consisted of same elements.

In the high-resolution spectra, the C 1s band contains four peaks, corresponding to sp^2 carbons (C=C, 284.4 eV), sp^3 carbons (C−O/C−N, 286 eV), carbonyl carbons (C=O, 287.7 eV), and carboxyl carbons (COOH, 289 eV) [41]. The N 1s band when deconvoluted, contains three peaks at 398.3, 399.2, and 400.2 eV, showing pyridinic N, amino N, and pyrrolic N, respectively. Interestingly, the yellow sample deconvoluted into a peak of oxidized N at 406.4 eV. The O 1s band contains two peaks at 531.7 and at 532.8 eV for C=O and C−O, respectively.

The XPS intensity at 289 eV (-COOH) increased slightly from sample A to sample C, suggesting an increment in the content of carboxyl groups on the surface of CDs and hence increased hydrophilicity (green and yellow) (**Table 4.1.**). Also, the intensity of the peak at 284.4 eV corresponding to C=C/C−C decreased from sample A to C indicating that sample A has the higher content nitrogen doped carbon atom network in the core. These variations are believed to be responsible for the different PL characteristics of the three CDs.

Samples	C=C /C−C	C−O/C−N	C=O	COOH
A	70%	25.8%	3.0%	1.2%
B	67.4%	25.3%	4%	3.3%
C	45%	31.3%	16.4%	7.3%

Table 4.1. XPS Data Analysis of the C 1s spectra of all 3 samples.

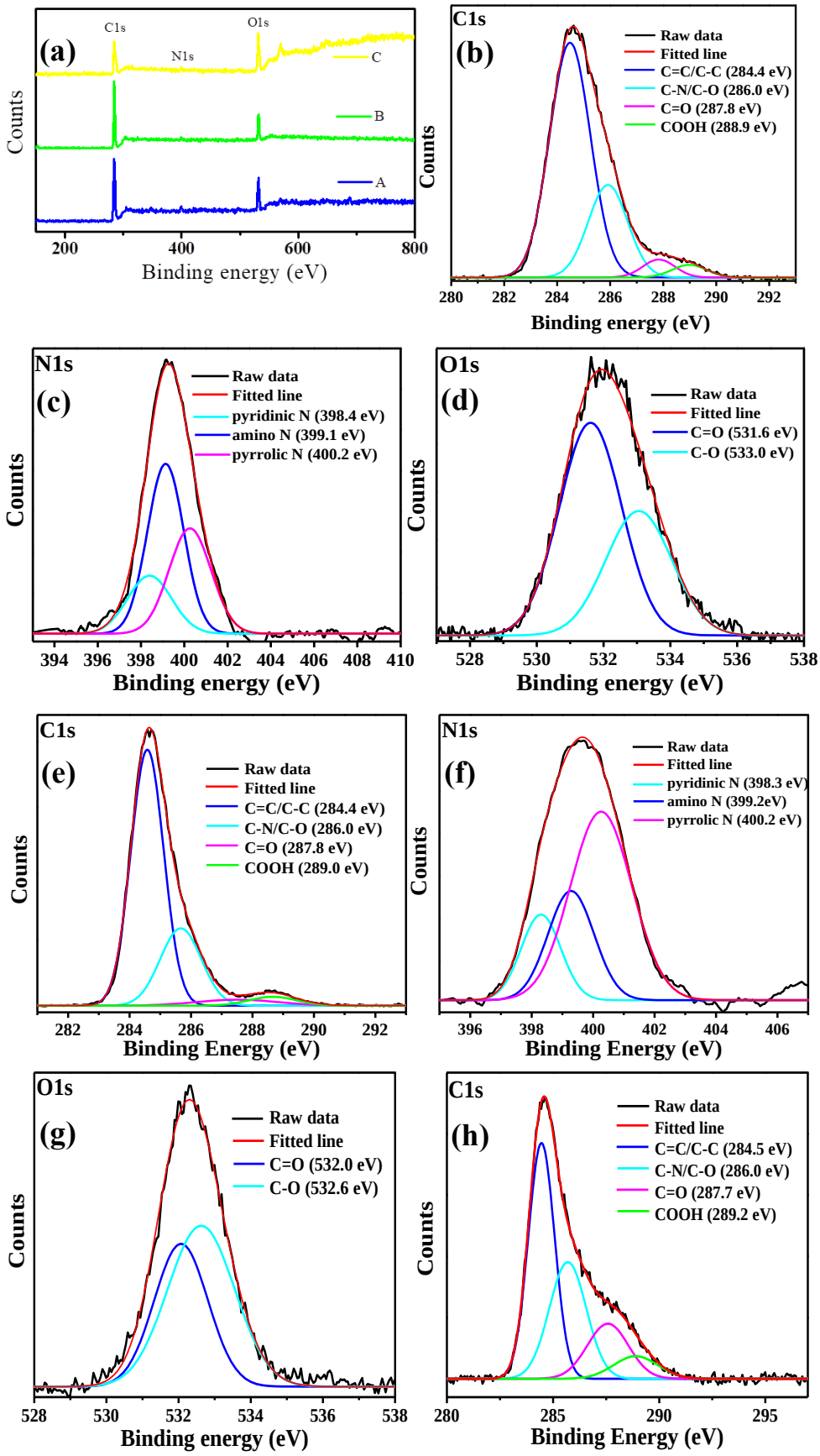
(a)
C1s
N1s
O1s
C
B
A
Counts
Binding energy (eV)
(b)
C1s
Raw data
Fitted line
C=C/C-C (284.4 eV)
C-N/C-O (286.0 eV)
C=O (287.8 eV)
COOH (288.9 eV)
Counts
Binding energy (eV)
(c)
N1s
Raw data
Fitted line
pyridinic N (398.4 eV)
amino N (399.1 eV)
pyrrolic N (400.2 eV)
Counts
Binding energy (eV)
(d)
O1s
Raw data
Fitted line
C=O (531.6 eV)
C-O (533.0 eV)
Counts
Binding energy (eV)
(e)
C1s
Raw data
Fitted line
C=C/C-C (284.4 eV)
C-N/C-O (286.0 eV)
C=O (287.8 eV)
COOH (289.0 eV)
Counts
Binding Energy (eV)
(f)
N1s
Raw data
Fitted line
pyridinic N (398.3 eV)
amino N (399.2eV)
pyrrolic N (400.2 eV)
Counts
Binding Energy (eV)
(g)
O1s
Raw data
Fitted line
C=O (532.0 eV)
C-O (532.6 eV)
Counts
Binding energy (eV)
(h)
C1s
Raw data
Fitted line
C=C/C-C (284.5 eV)
C-N/C-O (286.0 eV)
C=O (287.7 eV)
COOH (289.2 eV)
Counts
Binding Energy (eV)

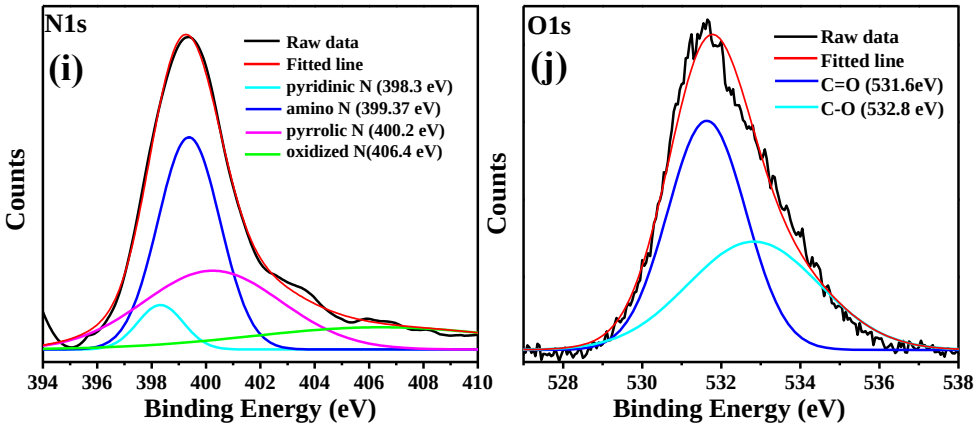

Figure 4.6. (a) XPS spectra of the three selected samples. (b, c and d) High-resolution XPS C 1s, N 1s, and O 1s spectra of sample A. (e, f and g) C 1s, N 1s, and O 1s spectra of sample B. (h, i and j) C 1s, N 1s, and O 1s spectra of sample C.

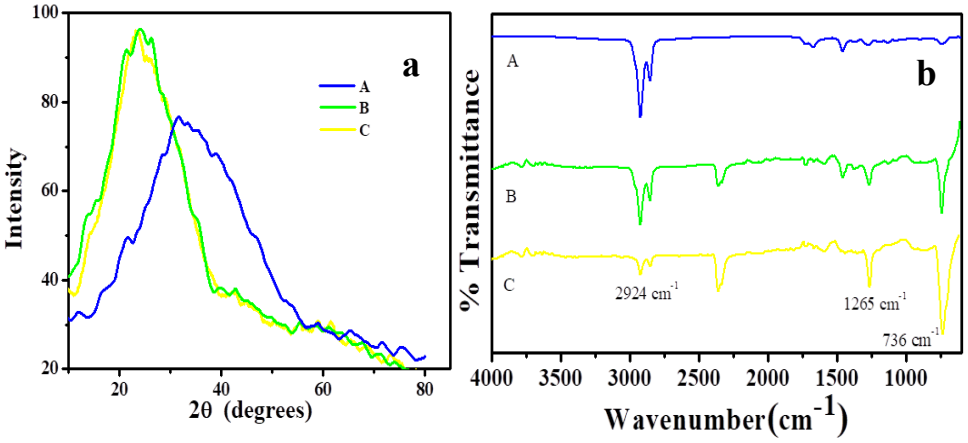

Figure 4.7. (a) XRD pattern of A, B and C. (b) FTIR spectra of three selected samples.

4.1.4. FTIR analysis

The Fourier Transform Infrared spectrum (FTIR) of the three carbon dots showed prominent peaks at 736 cm^{-1}, 1265 cm^{-1}, 1459 cm^{-1} and 1671 cm^{-1} which can be assigned to the stretching vibrations of o-substituted benzene, C-N, -C-N= and C=C respectively indicating the structures of polyaromatic structures of CDs during reaction process. No significant hydrogen bonded hydroxyl group was detected in any of the carbon dots (**Figure 4.7.b**).

A comparison of the FTIR spectra also shows that blue C-dots have maximum intensity of CH_2 and CH_3 stretching vibrations at 2924 and 2852 cm^{-1} respectively indicating presence of network of alkyl chains around the surface imparting hydrophobic characteristic to C-dots. This information is experimentally verified, as blue C-dots are least dispersible in water. The FTIR results are consistent with XPS analysis and we can conclude that the order of hydrophobicity is A>B>C.

4.1.5. X-ray diffraction pattern analysis

The diffraction peaks (**Figure 4.7.a**) of all the three CDs i.e. A (2θ = 31.81°), B (2θ = 24.14°) and C (2θ = 23.24°) are weak and broad as compared to the ordered structure of graphite (002 plane, 2θ = 26.5°). This signifies that sample A is highly amorphous as compared to B and C. The high *d* value in A indicates that other functional groups introduced in the synthetic process might have influenced in enhancement of the interlayer spacing.

4.1.6. TCSPC experiments

Time correlated single photon counting (TCSPC) experiments revealed that the average lifetime of blue, green and yellow samples were 0.997, 2.068 and 10.90 ns respectively (**Table 4.2.**).

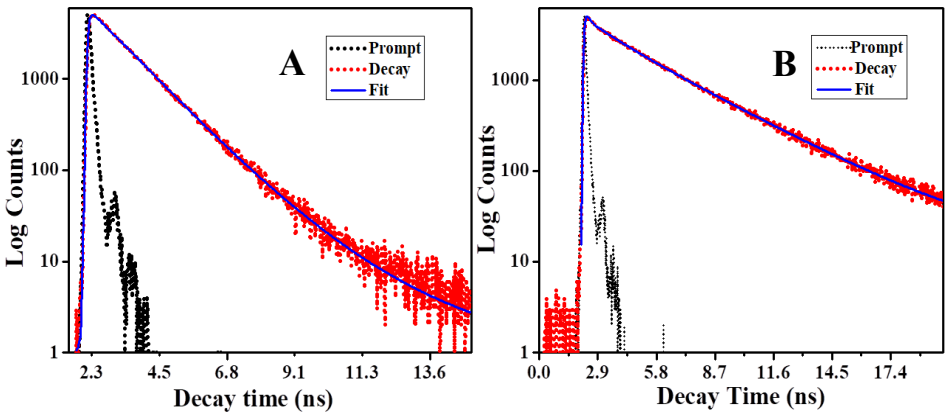

Figure 4.8. Fluorescence decay curves of sample A and B.

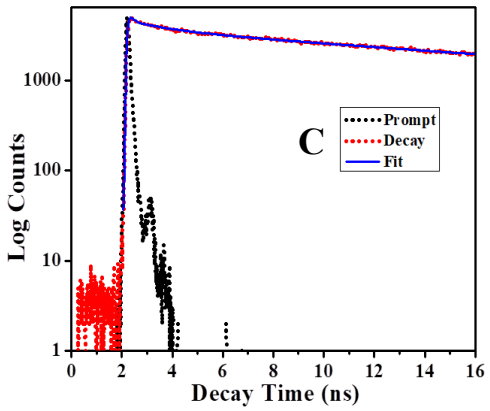

Figure 4.9. Fluorescence decay curve of sample C.

Samples	a_1	a_2	a_3	τ_1 (ns)	τ_2 (ns)	τ_3 (ns)	τ_{av} (ns)	χ^2
A	0	0.96	0.04	0	1.23	2.51	0.997	1.08
B	0.14	0.49	0.37	1.53	3.69	0.114	2.068	1.01
C	0.13	0.37	0.50	1.70	0.110	21.0	10.90	1.01

Table 4.2. Fluorescence lifetime studies of C-dots.

Plausible formation mechanism: Fumaric and maleic acid are stereoisomers. In fumaric acid, the two carboxylic acid groups are in trans configuration, wheras they are in cis form in maleic acid.

Solvothermal (ethanol) reaction at higher temperature favors the formation of different amide analogs between fumaric acid and o-phenylenediamine. Further condensation between $–NH_2$ and -COOH generates fused pyrrolic ring system. This phenomenon incorporates nitrogen into the graphitic core hence forming N-doped carbon dots (**Figure 4.11.**). Since, both $–NH_2$ and –COOH are involved in the water elimination, only a small amount of

surface functionalities from amines or carboxyl are detected in FTIR spectra. The formation of such polyaromatic alkyl network core doped with nitrogen imparts the hydrophobic character to the C-dots. Due to the difference in the number of conjugated double bonds, the PL emission varies from blue to peach.

In case of maleic acid, formation of fused pyrrolic ring system is hindered due to the proximity of both carboxylic acid group (**Figure 4.10.**). Hence, this pair did not generate a wider range of multicolor C-dots. The results suggest that the choice of precursors plays a critical role in the opto-electronic properties of the synthesized C-dots. It is generally believed that the surface functional groups contribute immensely into the emission behavior of the C-dots, as observed for several C-dots used for sensing of metal ions. However, we believe that in the present case, the amount of condensation between the fumaric acid and o-PD leading to the formation of carbon core, was instrumental in tuning the emission behavior. As observed, the condensation process was not homogeneous, leading to variable amount of nitrogen doped C-dots and alkyl chains in the core.

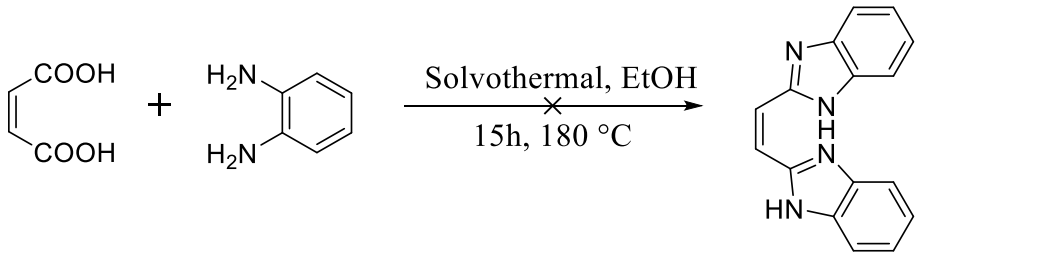

Figure 4.10. Plausible mechanism of hindrance in case of maleic acid (cis-isomer) and o-PD.

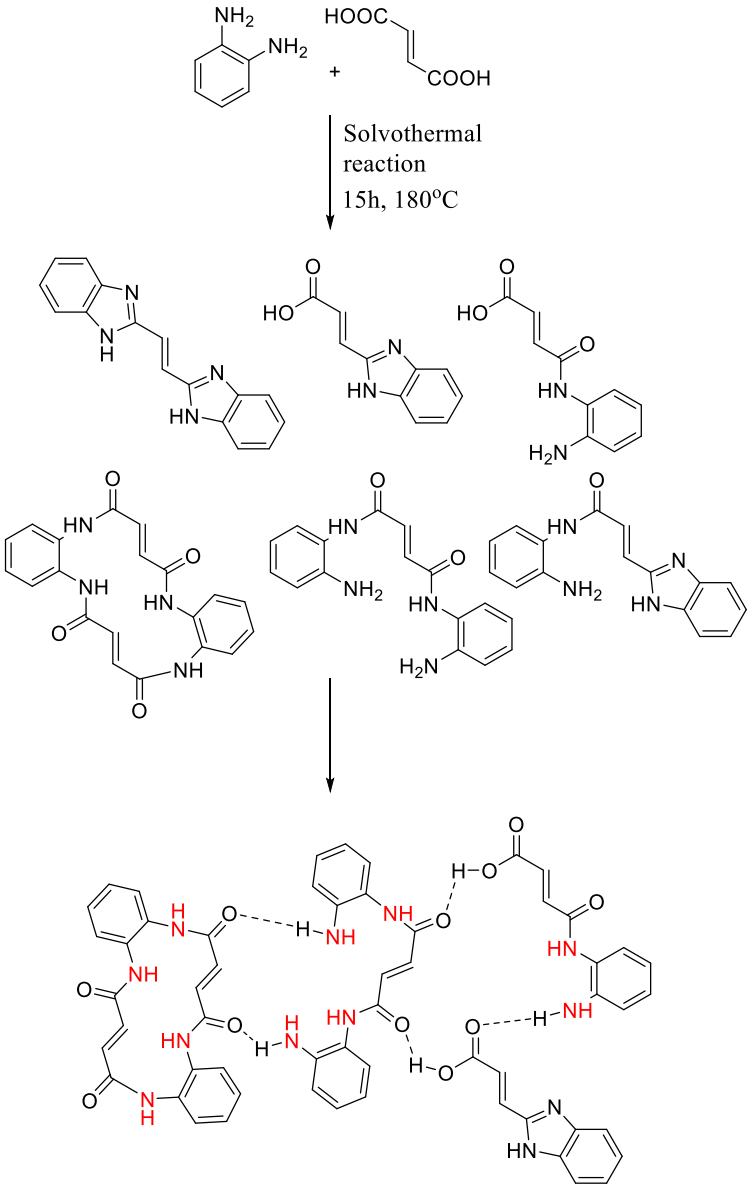

Figure 4.11. Possible mechanism for formation of N-doped C-dots.

4.2. Application of CDs: cell-imaging

4.2.1. Cell Culture

The HeLa cells (cervical cancer cell line) purchased from National Centre for Cell Science (NCCS), Pune, India were grown in DMEM culture medium with 10% heat-inactivated fetal bovine serum (FBS) and Pen-Strep solution (100 units/ml penicillin and 100units/ml streptomycin).

Media, FBS and Pen-strep solution were obtained from Life Technologies (Gaithersburg, MD, USA). HeLa Cells were seeded in 35 mm cell culture plates at a density of 3×104 cells/mL and were incubated at 37^{o}C in a 5% CO_2 humidified incubator for 2 h. Confocal images were acquired using laser scanning confocal microscopy (FV 1000, Olympus).

4.2.2. Cell imaging

The newly synthesized Carbon dots (blue, green and yellow) were further evaluated by performing *in vitro* studies using laser scanning confocal microscopy on HeLa cell lines (**Figure 4.12.**). After incubation for 2 h, the HeLa cells emitted strong blue, green and yellow fluorescence under illumination at a single wavelength of 488 nm. 10 μL of carbon dot was added to each well.

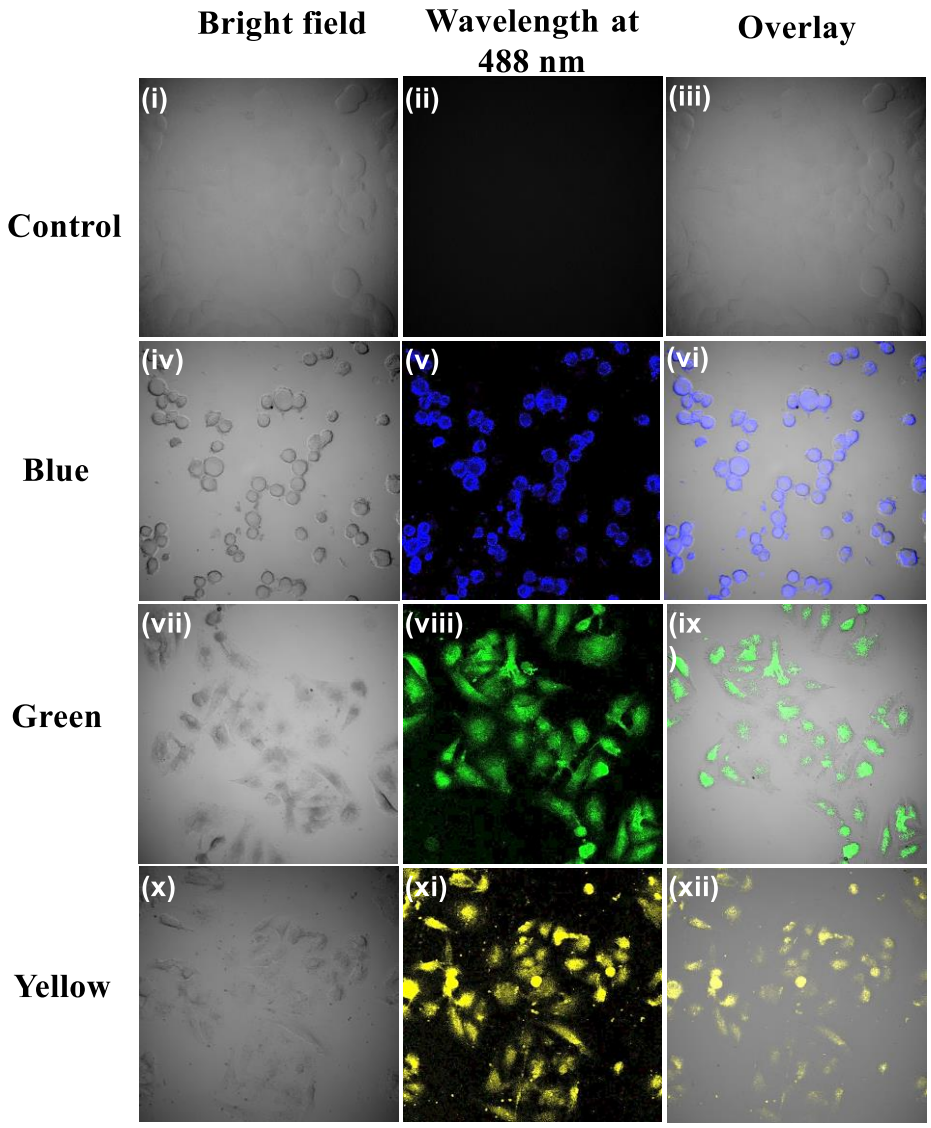

Figure 4.12. Panel (i) Bright field (DIC) image of HeLa cells for control experiment; Panel (iv), (vii), (x) bright field (DIC) image of HeLa cells with carbon dots (A, B and C) after 2h incubation; (ii) confocal image of control experiment at 488nm; Panel (v), (viii), (xi) uptake study by Confocal microscopy of HeLa cells with Carbon dots (A, B and C) after 2h incubation; Panel (iii), (vi), (ix) and (xii) represent the overlay images.

Chapter 5

Conclusion

In this thesis, a facile approach for the preparation of nitrogen doped carbon dots with high quantum yield is reported. The emission of the isolated C-dots is independent of the excitation wavelength and difference in the PL emission is proposed to be resulted from the difference in conjugation in the graphitic network containing N-atoms. Sized at approximately 2 nm, these C-dots show hydrophobic behavior as inferred from FTIR and XPS. Finally, all the three C-dots were applied for cell imaging with strong blue, green and yellow fluorescence emitted by HeLa cells. Overall, multi-color light emitting C-dots with high quantum yield and biocompatibility are prepared with potential application in bioimaging probes.

REFERENCES

1. Smalley R. E., Kroto H., Heath J., (1985), C60: Buckminsterfullerene, Nature, 318, 162−163.

2. Ruoff R. S., Tse D. S., Malhotra R., Lorents, D. C., (1993), Solubility of fullerene (C60) in a variety of solvents, J. Phys. Chem., 97, 3379-3383.

3. Iijima S., (1991), Helical Microtubules of Graphitic Carbon, Nature, 354, 56−58.

4. Novoselov K. S., Geim A. K., Morozov S. V., Jiang D., Zhang Y., Dubonos S. V., Grigorieva I. V., Firsov A. A., (2004), Electric field effect in atomically thin carbon films, Science, 306, 666−669.

5. Yan Q. L., Gozin M., Zhao F. Q., Cohen A., Pang S. P., (2016), Highly energetic compositions based on functionalized carbon nanomaterials, Nanoscale, 8, 4799-4851.

6. Liu Z., Robinson J. T., Tabakman S. M., Yang K., Dai H. J., (2011), Carbon materials for drug delivery & cancer therapy, Mater. Today, 14, 316−323.

7. Liang Y., Li Y., Wang H., Dai H., (2013), Strongly coupled inorganic/ nanocarbon hybrid materials for advanced electrocatalysis, J. Am. Chem. Soc., 135, 2013−2036.

8. Wang H. L., Dai H. J., (2013), Strongly coupled inorganic-nano-carbon hybrid materials for energy storage, Chem. Soc. Rev., 42, 3088−3113.

9. Da Ros T., Prato M., (1999), Medicinal chemistry with fullerenes and fullerene derivatives, Chem. Commun., 8, 663-669.

10. Bitounis D., Ali-Boucetta H., Hong B. H., Min D. H., Kostarelos K., (2013), Prospects and challenges of graphene in biomedical applications, Adv. Mater., 25, 2258-2268.

11. Ma P. C., Siddiqui N. A., Marom G., Kim J. K., (2010), Dispersion and functionalization of carbon nanotubes for polymer-based nanocomposites: a review, Compos. Part A Appl. Sci. Manuf., 41, 1345-1367.

12. Yan Q-L., Gozin M., Zhao F-Q., Cohen A., Pang S-P., (2016), Highly energetic compositions based on functionalized carbon nanomaterials, Nanoscale, 8, 4799-4851.

13. Baker S. N., Baker G. A., (2010), Luminescent Carbon Nanodots: Emergent Nanolights, Angew. Chem. Int. Ed., 49, 6726−6744.

14. Lim S. Y., Shen W., Gao Z., (2015), Carbon Quantum Dots and Their Applications, Chem. Soc. Rev., 44, 362−381.

15. Hola K., Zhang Y., Wang Y., Giannelis E. P., Zboril R., Rogach A. L., (2014), Carbon Dots-Emerging Light Emitters for Bioimaging, Cancer Therapy and Optoelectronics, Nano Today, 9, 590−603.

16. Wang, Y.; Hu, A. (2014) Carbon quantum dots: Synthesis, properties and applications. J. Mater. Chem. C, 2, 6921-6939.

17. Li, H., Kang, Z., Liu, Y., Lee, S.T., (2012), Carbon nanodots: Synthesis, properties and applications, J. Mater. Chem., 22, 24230-24253.

18. Shen J., Zhu Y., Yang X., Li C., (2012), Graphene quantum dots: Emergent nano- lights for bioimaging, sensors, catalysis and photovoltaic devices, Chem. Commun., 48, 3686-3699.

19. Xu X. Y., Ray R., Gu Y. L., Ploehn H. J., Gearheart L., Raker K., Scrivens W. A., (2004), Electrophoretic analysis and purification of

fluorescent single-walled carbon nanotube fragments, J. Am. Chem. Soc., 126, 12736−12737.

20. Zhu S., Song Y., Zhao X., Shao J., Zhang J., Yang B., (2015), The photoluminescence mechanism in carbon dots (graphene quantum dots, carbon nanodots, and polymer dots): Current state and future perspective, Nano Res., 8, 355-381.

21. Baker S. N., Baker G. A., (2010), Luminescent carbon nanodots: Emergent nanolights, Angew. Chem. Int. Ed., 49, 6726-6744.

22. Bourlinos A. B., Stassinopoulos A., Anglos D., Zboril R., Karakassides M., Giannelis E. P., (2008), Surface functionalized carbogenic quantum dots, Small, 4, 455-458.

23. Ye R., Xiang C., Lin J., Peng Z., Huang K., Yan Z., Ceriotti G., (2013), Coal as an abundant source of graphene quantum dots, Nat. Commun., 4, 2943.

24. Wang J., Wang C. F., Chen S., (2012), Amphiphilic egg-derived carbon dots: Rapid plasma fabrication, pyrolysis process and multicolor printing patterns, Angew. Chem. Int. Ed., 51, 9297-9301.

25. Jiang J., He Y., Li S., Cui H., (2012), Amino acids as the source for producing carbon nanodots: Microwave assisted one-step synthesis, intrinsic photoluminescence property and intense chemiluminescence enhancement, Chem. Commun., 48, 9634-9636.

26. Zhu S., Meng Q., Wang L., Zhang J., Song Y., Jin H., Zhang K., Sun H., Wang H., Yang B., (2013), Highly photoluminescent carbon dots for multicolor patterning, sensors, and bioimaging, Angew. Chem. Int. Ed., 52, 3953-3957.

27. Li H., He X., Kang Z., Huang H., Liu Y., Liu J., Lian S., Tsang C.H., Yang X., Lee S. T., (2010), Water-soluble fluorescent carbon quantum dots and photocatalyst design, Angew. Chem. Int. Ed., 49, 4430-4434.

28. De B., Karak N., (2017), Recent progress in carbon dot–metal based nanohybrids for photochemical and electrochemical applications, J. Mater. Chem. A, 5, 1826-1859.

29. Barman M. K., Jana B., Bhattacharyya S., Patra A., (2014), Photophysical properties of doped carbon dots (N, P, and B) and their influence on electron/hole transfer in carbon dots–nickel (II) phthalocyanine conjugates, J. Phys. Chem. C, 118, 20034-20041.

30. Lu Y., Zhang L., Lin H., (2014), The use of a microreactor for rapid screening of the reaction conditions and investigation of the photoluminescence mechanism of carbon dots, Chem. Eur. J., 20, 4246−4250.

31. Nie H., Li M., Li Q., Liang S., Tan Y., Sheng L., Shi W., Zhang S. X. A., (2014), Carbon Dots with continuously tunable full-color emission and their application in ratiometric pH sensing, Chem. Mater., 26, 3104−3112.

32. Zhai X., Zhang P., Liu C., Bai T., Li W., Dai L., Liu W., (2012), Highly luminescent carbon nanodots by microwave-assisted pyrolysis, Chem. Commun., 48, 7955−7957.

33. Hu S., Trinchi A., Atkin P., Cole, I., (2015) Tunable photo-luminescence across the entire visible spectrum from carbon dots excited by white light, Angew. Chem. Int. Ed., 54, 2970−2974.

34. Jiang K., Sun S., Zhang L., Lu Y., Wu A., Cai C., Lin H., (2015), Red, green, and blue luminescence by carbon dots: Full-color emission tuning and multicolor cellular imaging, Angew. Chem. Int. Ed., 54, 5360−5363.

35. Bao L., Liu C., Zhang Z. L., Pang D. W., (2015), Photoluminescence-tunable carbon nanodots: Surface-state energy-gap tuning, Adv. Mater., 27, 1663−1667.

36. Ding H., Wei J. S., Xiong H. M., (2014), Nitrogen and sulfur co-doped carbon dots with strong blue luminescence, Nanoscale, 6, 13817−13823.

37. Krysmann M. J., Kelarakis A., Dallas P., Giannelis E. P., (2012) Formation mechanism of carbogenic nanoparticles with dual photoluminescence emission, J. Am. Chem. Soc., 134, 747−750.

38. Zhu S., Song Y., Zhao X., Shao J., Zhang J., Yang B., (2015), The photoluminescence mechanism in carbon dots (Graphene Quantum dots, Carbon Nanodots, and Polymer Dots): Current state and future Perspective, Nano Res., 8, 355−381.

39. Zhu S., Meng Q., Wang L., Zhang J., Song Y., Jin H., Zhang K., Sun H., Wang H., Yang B., (2013), Highly photoluminescent carbon dots for multicolor patterning, sensors, and bioimaging, Angew. Chem. Int. Ed., 52, 3953−3957.

40. Song L., Cui Y., Zang, C., Hu Z., Liu X., (2016), Microwave-assisted facile synthesis of yellow fluorescent carbon dots from o-phenylenediamine for cell imaging and sensitive detection of Fe^{3+} and H_2O_2, RSC Adv., 6, 17704–17712.

41. Ding H., Yu S., Wei J., Xiong H., (2016), Full-Color light-emitting carbon dots with a surface-state-controlled luminescence mechanism, ACS Nano, 10, 484−491.